Volume 34 (July 2024), 176–187

Herpetological Journal

FULL PAPER

https://doi.org/10.33256/34.3.176187

Published by the British Herpetological Society

Larval morphology, vocalisations, and phylogenetic position of *Crossodactylus dantei* (Anura: Hylodidae): new insights into a little-known anuran species

Gustavo Fernandes Telles Moreira[1,2], Barnagleison Silva Lisboa[2,3], Marcos Jorge Matias Dubeux[1,2,4], Jessika Maria de Moura Neves[1,2], Tamí Mott[1,2] & Filipe Augusto Cavalcanti do Nascimento[1,2]

[1]Laboratório de Biologia Integrativa, Setor de Biodiversidade, Instituto de Ciências Biológicas e da Saúde, Universidade Federal de Alagoas, Maceió, Brazil

[2]Setor de Herpetologia, Museu de História Natural, Universidade Federal de Alagoas, Maceió, Brazil

[3]Instituto Federal de Alagoas, Campus Santana do Ipanema, Santana do Ipanema, Brazil

[4]Programa de Pós-Graduação em Biologia Animal, Centro de Biociências, Departamento de Zoologia, Universidade Federal de Pernambuco, Recife, Brazil

Aspects of the biology and natural history of the endemic anuran *Crossodactylus dantei* remain unknown even almost 30 years since its description. In this study, we describe its larval stage, along with the advertisement and territorial calls, and assess its phylogenetic positioning based on a fragment of the 16S rRNA mitochondrial gene. The larval stage of *C. dantei* follows the morphological pattern of Hylodidae, corroborating the relatively uniform larval morphology of the family. However, it is still possible to observe characters that distinguish *C. dantei* from other species in the genus, such as the elliptical body in dorsal view, nostrils located closer to the snout than to the eyes, an elongated pre-nasal arena, and the absence of taenia tecti medialis and taenia tecti transversalis in the chondrocranium. Its advertisement call is characterised by a sequence of about 23 pulsed notes, with ascending amplitude modulation, and has a mean duration of 2.5 seconds, with a dominant frequency of 3356 Hz. The territorial call has a mean duration of 23 seconds, a dominant frequency of 3160 Hz, and two distinct types of notes. Phylogenetic analysis indicated the existence of two main lineages in the genus. *Crossodactylus dantei* was recovered with high statistical support as a sister species to the clade composed of *C. gaudichaudii* and *C. timbuhy*. Furthermore, the group formed by these three species was recovered as the sister lineage of *C. trachystomus*. In summary, the information presented here represents a significant advance in the knowledge of this enigmatic and rare species of the northern Atlantic Forest, providing baseline data for future ecological and evolutionary studies of this unique frog.

Keywords: tadpole, oral anatomy, chondrocranium, calls, phylogeny, Atlantic Forest

INTRODUCTION

The family Hylodidae encompasses diurnal anuran amphibians that primarily inhabit flowing freshwater environments in the Atlantic Rainforest (Caldart et al., 2012). Its geographical distribution ranges from north-eastern to southern Brazil and northern Argentina (Caldart et al., 2012; Laia & Rocha, 2012). Currently, this family comprises a total of 48 recognised species, classified into four genera: *Crossodactylus* Duméril & Bibron, 1841; *Megaelosia* Miranda-Ribeiro, 1923; *Hylodes* Fitzinger, 1826; and *Phantasmarana* Vittorazzi, Augusto-Alves, Neves-da-Silva, Carvalho-e-Silva, Recco-Pimentel, Toledo, Lourenço & Bruschi, 2021. Among these, *Crossodactylus* stands as the second most diverse, with 13 species distributed from north-eastern Brazil to the province of Misiones in Argentina (Frost, 2023).

Crossodactylus demonstrates a strong association with habitats characterised by mountainous and rocky terrain (Pimenta et al., 2014), presenting significant challenges for research efforts. Notably, some species were last collected during the latter part of the 20th century (*C. boulengeri* (De Witte, 1930); *C. dispar* Lutz, 1995; *C. grandis* Lutz, 1951, and possibly others), raising concerns about their potential extinction (Pimenta et al., 2014). Their taxonomic relationships remain problematic, and a limited number of studies have been conducted on *Crossodactylus* phylogenetics, where only a small subset of the current recognised species within the genus were included, i.e. *C. caramaschii* Bastos & Pombal, 1995; *C. gaudichaudii* Duméril & Bibron, 1841; *C. schmidti* Gallardo, 1961; *C. trachystomus* (Reinhardt & Lütken, 1862); and *C. werneri* Pimenta, Cruz & Caramaschi, 2014 (e.g. Toscano et al., 2019; Vittorazzi et al., 2021; de Sá et al., 2022).

Consequently, our understanding of other biological aspects pertaining to this group remains deficient, hindering conservation efforts. The acoustic repertoire

Correspondence: Gustavo Moreira (moreira.gustavotelles@gmail.com)

of the genus is under-studied, where advertisement calls have only been documented for little more than half of the *Crossodactylus* diversity (i.e. *C. caramaschii*; *C. cyclospinus* Nascimento, Cruz & Feio, 2005; *C. franciscanus* Pimenta, Caramaschi & Cruz, 2015; *C. gaudichaudii*, *C. schmidti*, *C. timbuhy* Pimenta, Cruz & Caramaschi; *C. trachystomus* and *C. werneri*). Additionally, only seven species have documented tadpole morphologies, primarily limited to external features (i.e. *C. caramaschii*, *C. cyclospinus*, *C. gaudichaudii*, *C. schmidti*, *C. timbuhy*, *C. trachystomus* and *C. werneri*); detailed accounts of the buccopharyngeal cavity, a set of features critical to feeding ecology (Wassersug, 1976; Candioti, 2007), have been recorded for merely three species (*C. caramaschii*, *C. gaudichaudii* and *C. trachystomus*); while data about the larval skeleton, i.e. the chondrocranium and hyobranchial apparatus, both of significant systematic and phylogenetic value (e.g. Larson & de Sá, 1998; Vera Candioti, 2007), exists for just one species (*C. gaudichaudii*).

Crossodactylus dantei Carcerelli & Caramaschi, 1993 is an endemic anuran species found in the municipality of Murici, State of Alagoas, north-east Brazil. This species is the only Hylodidae known to occur in the northern portion of the Atlantic Forest (Vieira et al., 2023). Its occurrence is restricted to a small range of only 8 km² and its presence has only been recorded in two streams. For over two decades (1988–2012) there were no recorded sightings of this species, and except for the adult description, there is no data about its biology or natural history. Currently, the IUCN Red List of Threatened Species designates *C. dantei* as Data Deficient (IUCN, 2004).

Herein, we provide the first description of larval morphology, and the advertisement and territorial calls of *C. dantei*; in addition, we assess its phylogenetic positioning.

MATERIALS & METHODS

Tadpole morphology

We analysed twelve tadpoles at stages 25, 37 and 44 (Gosner, 1960) housed at the Herpetological Collection of the Museu de História Natural of the Universidade Federal de Alagoas (MHNUFAL 12051–54). The specimens were collected at the species' type locality (Mata da Bananeira, 9° 12'00" S, 35° 52'00" W, DATUM WGS84; 551 m a.s.l., Estação Ecológica de Murici, municipality of Murici, Alagoas State, Brazil), anesthetised with 5% lidocaine, then fixed and preserved in 10% formalin (commercial grade).

For the external morphology, 28 measurements were taken. These measurements followed McDiarmid & Altig (1999) for total length (TL), body length (BL), maximum tail height (MTH), tail length (TaL), tail muscle height (TMH), and tail muscle width (TMW); Lavilla & Scrocchi (1986) for body width at eye level (BWE), body width at nostril level (BWN), dorsal gap of the oral disc width (DGO), extranarial distance (EnD), extraorbital distance (EoD), eye diameter (ED), eye-nostril distance (END), intranarial distance (InD), intraorbital distance (IoD), maximum body height (MBH), maximum body width (MBW), narial diameter (ND), oral disc width (ODW), snout-nostril distance (SND), snout-spiracle distance (SSD) and spiracle-posterior body distance (SPD); Grosjean (2005) for dorsal fin height (DFH) and ventral fin height (VFH); Rodrigues et al. (2017) for spiracle length (SL) and vent tube length (VTL); Pinheiro et al. (2012) for dorsal fin insertion angle (DFIA) and Altig & Johnson (1989) for angular orientation of the oral disc (ODAO). Measurements were taken using an ocular micrometer installed on a Coleman® XTB/2B stereomicroscope, with the exception of total length, which was measured using a digital caliper with an accuracy of 0.1 mm. The insertion angle of the dorsal fin and the angular orientation of the oral disc were measured using ImageJ v. 1.50i software, through photos captured with a digital camera coupled with a stereomicroscope. Terminology followed McDiarmid & Altig (1999).

Descriptions of the buccopharyngeal cavity were based on two tadpoles at stage 25 (MHNUFAL 12054), which were dissected following Wassersug (1976) to expose the buccal roof and floor. Subsequently, they were stained with methylene blue and lugol solution, observed and characterised under a stereomicroscope. Terminology followed Wassersug (1976; 1980).

Descriptions of the larval skeleton were based on two tadpoles at stage 25 (MHNUFAL 12051, 12054). Specimens were cleaned and double-stained for bone and cartilage following the protocol of Dingerkus & Uhler (1977). They were observed and characterised under a stereomicroscope. Terminology followed Larson & de Sá (1998) and Haas (2003).

Bioacoustics data

Field expeditions were conducted between December 2012 and December 2013 at the species' type locality. On 31 May 2013 a male was observed calling above partially submerged leaves at the edge of a small permanent stream. The calls were recorded using a Marantz® PMD 660 digital recorder coupled with a Sennheiser® K6/ME66 directional microphone from a distance of about 1 m between 11:00 h – 13:00 h (air temperature = 24.2 °C, water temperature = 23.4 °C, and relative humidity = 90%). The recordings were sampled at 44 kHz and 16 bits resolution.

Data analysis was performed using the software Raven Pro 1.6.4 for Windows (Cornell Lab of Ornithology, Bioacoustics Research Program, 2023). Spectrograms were created using Seewave package version 2.2.0 (Sueur et al., 2008) in the software R version 4.2.1 (R Core Team, 2022), with Hann window, FFT size of 512 points, and 90% overlap. The calls were classified based on observations of the frogs' social context in the field (Wells, 2007). The temporal and spectral parameters analysed included: calls per minute, call duration, intercall interval, notes per call, note duration, pulses per note, internote interval and dominant frequency; terminology follows Köhler et al. (2017).

Call voucher specimens were deposited in the herpetological collection of the Museu de História Natural, Universidade Federal de Alagoas (MHNUFAL 11934). The acoustic recordings are housed in the Fonoteca Zoológica Gabriel Skuk of the Museu de História Natural (MHNUFAL-SOM 054–056).

Figure 1. *Crossodactylus dantei* tadpole (MHNUFAL 17664) at stage 25 (Gosner, 1960). **(A)** Lateral, **(B)** dorsal and **(C)** ventral views (scale bar = 10 mm); **(D)** oral disc (scale bar = 1 mm).

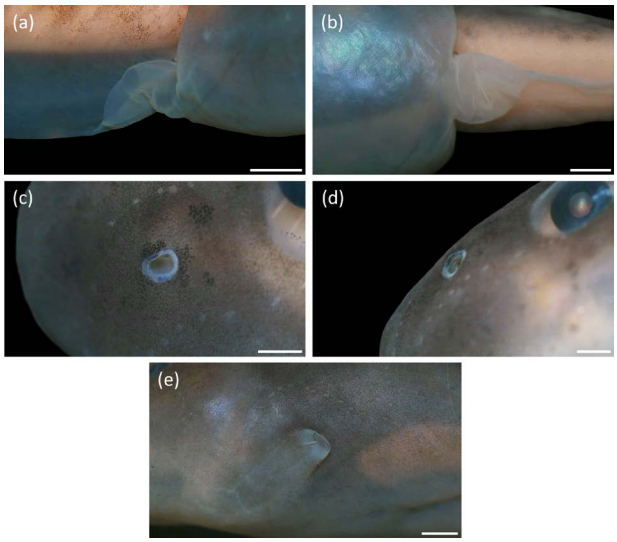

Figure 2. *Crossodactylus dantei* tadpole (MHNUFAL 12054) at stage 25 (Gosner, 1960; scale bar = 1 mm). Vent tube in **(A)** lateral and **(B)** ventral views; left nostril in **(C)** dorsolateral and **(D)** lateral views; **(E)** spiracle in lateral view.

Molecular data

Genomic DNA was extracted from the tail muscle tissue of a tadpole collected at the type-locality (MHNUFAL 17664), utilising the Phenol/Chloroform method (Sambrook et al., 1989). Extracted DNA was quantified and purity was assessed through a Loccus® L-Quant spectrophotometer. Amplification of a 418-base pair fragment of the mitochondrial 16S rRNA gene was performed via Polymerase Chain Reaction (PCR) employing An16SF and An16SR primers (Lyra et al., 2017). The presence of amplicons was verified through electrophoresis in a 1% agarose gel stained with Sybr® Safe and visualised under ultraviolet light on a Vilber Lourmat® transilluminator. Subsequently, the sample was purified with isopropanol and sent to ACTGENE - Molecular Analysis (Alvorada, Brazil) for forward sequencing.

The sequenced material was edited with BioEdit v. 7.0.9 (Hall, 1999) and aligned using the software MAFFT v7.490 (Katoh & Standley, 2013) with representative samples of all Hylodidae and Alsodidae genera (sensu Grant, 2019) available in GenBank. Additionally, a sequence of *Cycloramphus boraceiensis* (Heyer, 1983) was used to root the phylogeny. The final molecular dataset comprised a total of 170 individuals, representing 50 species (See Table S1 in supplementary material for GenBank accession numbers). The best evolutionary model was determined using PartitionFinder 2.1.1 (Lanfear et al., 2012), considering all search algorithms, branches as connected, and using the Bayesian information criterion as the selection method. Two independent Bayesian Inference analyses were performed using MrBayes 3.2 software (Ronquist et al., 2012), with ten million generations and sampling every 1000 generations. A majority consensus tree was generated to obtain the final topology after discarding 25% of the initial trees. The Kimura-2-parameter evolutionary model (K2P; Kimura, 1980) was utilised, with complete gap deletion, to calculate the genetic distances both within and between species using the MEGA X software (Kumar et al., 2018).

RESULTS

Tadpole external morphology

Total length 43.7 ± 4.7 mm (34.3–48.8 mm). Body elliptical in dorsal and ventral views (MBW/BL = 0.49–0.65), globular-depressed in lateral view (MBH/MBW = 0.66–0.90), ventral contour convex, constriction at spiracle level present (Fig. 1A–C). Body length about 38% of total length (BL/TL = 0.35–0.42), greatest height varying between middle or posterior third of body, greatest width in the middle third of body. Tip of snout circular in lateral and dorsal views. Eyes dorsal, laterally oriented (ED/BWE = 0.12–0.21), occupying 50% of intraorbital distance (ED/IOD = 0.37–0.71), and representing 15% of maximum body width (ED/MBW = 0.12–0.19). Nostrils elliptical, dorsally located, directed laterally or anterodorsally, bearing a small flap at the medial margin; represents 16% of the intranarial distance (ND/InD = 0.10–0.23), 5% of the maximum body width (ND/MBW = 0.04–0.07), and 7% of body width at nostril level (ND/BWN = 0.05–0.10), maximum length parallel to longitudinal body axis, located closer to snout than eyes (END/SND = 0.75–1.36), openings leveled with surrounding surface (Fig. 2C & D). Spiracle single, sinistral, located below the midline at the middle third of the body (SPD/SSD = 0.62–0.88), visible in dorsal and ventral views, posterodorsally directed, inner wall presents as a small ridge, external wall ending anteriorly

to the inner wall (Fig. 2E). Vent tube dextral, attached to the ventral fin, with dextral membrane displaced dorsally and anteriorly, opening smooth (Fig. 2A & B). Tail length approximately 62% of total length (TaL/TL = 0.57–0.64), maximum height at the middle third of the tail, maximum height exceeding maximum body height (MBH/MTH = 0.67–0.99), tail tip varying between narrowly rounded to pointed. Tail musculature robust, maximum height approximately half of the maximum tail height (TMH/MTH = 0.38–0.55), progressively thinner as it approaches the posterior end, myosepta distinct along its entire length. Dorsal fin height greater than ventral fin height (VFH/DFH = 0.65–0.84), less than half of the maximum tail height (DFH/MTH = 0.33–0.45), maximum height in its middle third; originates at the body-tail junction at a narrow angle (DFIA = 2.90°–6.40°), continuing almost parallel to the tail musculature, it has a semicircle outline up to the posterior third, where it abruptly converges to the tail tip. Ventral fin begins at the ventral end of the body, maximum height in the anterior third, semicircle outline that slightly converges towards the end of the tail. Oral disc equivalent to 39% of the maximum body width (ODW/MBW = 0.33–0.50), ventrally positioned (ODAO = 20.14°–26.17°), laterally emarginated; bordered by a single row of marginal papillae (12 papillae/mm), except for its anterior margin, which presents a dorsal-medial gap equivalent to 53% of oral disc width (DGO/ODW = 0.46–0.60); papillae have conical or rounded tips and no pigmentation; submarginal papillae present, irregularly distributed along the sides of the oral disc (Fig. 1D). Labial tooth row formula (LTRF) 2(2)/3(1), P3 20% smaller than the other rows and P2 with medial indentation, A2 and P1 with medial gaps (30% of the length of A1 and 20% of the length of P2, respectively). Jaw-sheaths pigmented; upper jaw-sheath arch shaped with finely serrated margins, bearing a medial projection; lower jaw-sheath 'V' shaped and robust. A summary of tadpoles' measurements is provided in Table 1.

Colouration in preservative: anterior portion of the dorsum beige, transitioning to a dark brown in the middle third, peribranchial and abdominal regions translucent, with light brown/grey at sides; shapeless melanophores scattered irregularly across the initial portion of the anterior third of the body, which crosses the body dorsally up to the base of the tail. Fins translucent, with brown musculature on its anterior third, that becomes translucent as it approaches the end of the tail; shapeless melanophores are irregularly scattered throughout the tail, except for the anterior and middle thirds of the ventral fin. At the end of metamorphosis, stage 44, the dorsum and laterals of the body become brown, the ventral side area milky white, and the melanophores disappear from the body, remaining only on the tail.

Lateral line system (Fig. 3): supraorbital line composed of 12–21 stitches beginning posteromedially to the eyes and converging dorsally towards the snout, contouring the nostril and ending above the oral disc; infraorbital line composed of 15–20 stitches that starts posteromedially to the eyes, just below the beginning of the supraorbital line, and runs anterolaterally towards the snout, ending above the oral disc; posterior supraorbital line composed of 2–7 stitches that occurs posterior to the supraorbital line; posterior infraorbital line composed of 3–4 stitches located posterolaterally to the infraorbital line; angular line composed of 9–13 stitches that starts laterally to the infraorbital line, then runs ventrally, ending at the plane of the spiracle; oral longitudinal line has 7–12 stitches that starts laterally to the oral disc and runs laterally through the body until near the nostrils; ventral line

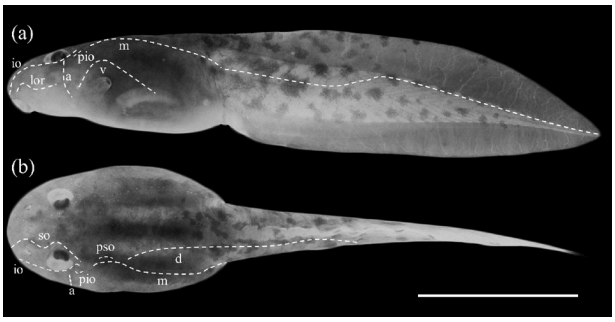

Figure 3. Lateral line system of *Crossodactylus dantei* (scale = 10 mm). Abbreviations: a = angular line; d = dorsal line; io = infraorbital line; lor = oral longitudinal line; m = medial line; pio = posterior infraorbital line; pso = posterior supraorbital line; so = supraorbital line; v = ventral line.

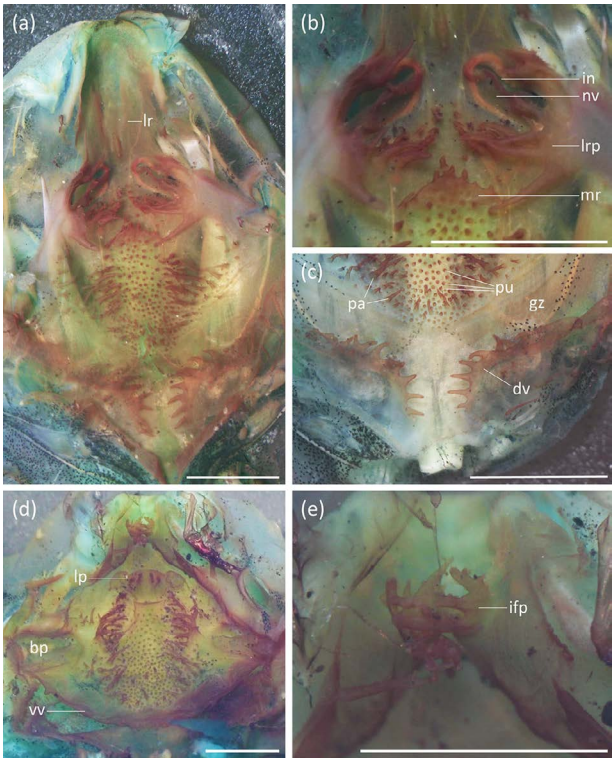

Figure 4. Buccal roof **(A–C)** and floor **(D–E)** of *Crossodactylus dantei* (MHNUFAL 12054) at stage 25 (Gosner, 1960; scale bar = 1 mm). Abbreviations: bp = buccal pockets; dv = dorsal velum; gz = glandular zone; ifp = infralabial papillae; in = internal nare; lp = lingual papillae; lr = longitudinal ridges; lrp = lateral ridge papillae; mr = median ridge; nv = narial valve; pa = papillae; pu = pustules; vv = ventral velum.

Table 1. Measurements (in mm; DFIA and ODAO in degree) of *Crossodactylus dantei* tadpoles (lots MHNUFAL 12051, 12052, 12053, 12054). Data presented as mean ± standard deviation (range). Stages according to Gosner (1960).

Measurements	Stage 25 (N = 8)	Stage 37 (N = 2)	Stage 44 (N = 2)
Total length	43 ± 5 (34.3-48.8)	46.8 ± 1.7 (45.6-48.1)	23.4 ± 0.2 (23.3-23.6)
Body length	16.1 ± 2.1 (13.1-18.6)	18.5 ± 1.3 (17.6-19.4)	15.5 ± 0.1 (15.4-15.5)
Maximum body width	9.2 ± 1.4 (6.5-10.7)	11 ± 0.3 (10.8-11.2)	5.9 ± 0.4 (5.6-6.3)
Body width at eyes level	8.7 ± 1 (7.2-10)	9.9 ± 0.7 (9.4-10.4)	6.4 ± 0.4 (6.1-6.6)
Body width at the nostril level	6.6 ± 0.7 (5.4-7.5)	6.9 ± 0.1 (6.8-7)	2.9 ± 0.1 (2.8-2.9)
Maximum body height	7.2 ± 1.2 (5.1-8.5)	9.7 ± 0.1 (9.6-9.8)	5.5 ± 0.5 (5.1-5.9)
Extraorbital distance	6.1 ± 0.8 (5.4-7.4)	6.7 ± 0.2 (6.5-6.8)	6.3 ± 0.5 (5.9-6.6)
Intraorbital distance	3 ± 0.4 (2.3-3.7)	3 ± 0.2 (2.8-3.1)	5.1 ± 0.4 (4.8-5.3)
Eye diameter	1.3 ± 0.2 (1-1.6)	2.1 ± 0.1 (2-2.2)	1.7 ± 0 (1.7-1.7)
Extranarial distance	3.8 ± 0.5 (3-4.5)	4.4 ± 0 (4.4-4.4)	3 ± 0.1 (2.9-3)
Intranarial distance	3 ± 0.6 (2.1-3.9)	3.6 ± 0.4 (3.3-3.8)	2.5 ± 0.1 (2.4-2.5)
Narial diameter	0.5 ± 0.1 (0.3-0.8)	0.5 ± 0 (0.5-0.5)	0.3 ± 0.1 (0.2-0.3)
Eye-nostril distance	1.6 ± 0.2 (1.2-2)	1.6 ± 0.1 (1.5-1.6)	1.4 ± 0.1 (1.3-1.4)
Snout-nostril distance	1.8 ± 0.3 (1.1-2.1)	1.7 ± 0.3 (1.5-1.9)	0.6 ± 0.1 (0.5-0.6)
Snout-spiracle distance	9.7 ± 0.9 (8.2-11)	10.2 ± 0.9 (9.5-10.8)	
Spiracle-posterior body distance	7.4 ± 1.1 (5.5-8.8)	8.8 ± 0.9 (8.1-9.4)	
Spiracle length	1.7 ± 0.5 (1.2-2.5)	2.1 ± 0.1 (2-2.1)	
Vent tube length	2.5 ± 0.4 (2-2.9)	3.5 ± 0.7 (3-4)	
Oral disk width	3.7 ± 0.4 (3-4.2)	4.1 ± 0.1 (4-4.2)	
Width of the dorsal gap of the oral disk	2 ± 0.3 (1.7-2.6)	2.1 ± 0.3 (1.9-2.3)	
Tail length	26.9 ± 3.2 (21.2-31.7)	28.4 ± 3 (26.2-30.5)	8 ± 0.1 (7.9-8.1)
Maximum tail height	9.2 ± 1.3 (7.1-10.4)	10.2 ± 0.5 (9.8-10.5)	3 ± 0.4 (2.7-3.2)
Tail muscle height	4.8 ± 1.1 (2.9-6.3)	5.7 ± 0.5 (5.3-6)	4.5 ± 0.1 (4.4-4.5)
Tail muscle width	4.2 ± 0.8 (2.9-5.4)	5.4 ± 0 (5.4-5.4)	3 ± 0.4 (2.7-3.2)
Dorsal fin height	3.4 ± 0.6 (2.5-4)	4.1 ± 0.4 (3.8-4.3)	
Ventral fin height	2.6 ± 0.4 (2-3)	3 ± 0.2 (2.8-3.1)	
Dorsal fin insertion angle	4.3° ± 1.3° (2.9°-5.6°)	5.2° ± 1.6° (4°-6.4°)	12.1° ± 4.8° (8.7°-15.6°)
Oral disk angular orientation	23.2° ± 2.7° (20.14°-25.42°)	25.9° ± 0.3° (25.6°-26.1°)	

composed of 18–23 stitches that starts on the anterior portion of the body at the plane of the spiracle, runs posterodorsally and then converges ventrally, in a way to circle the spiracle, ending posteriorly to it but at the same plane where the line started; dorsal line composed of 19–25 stitches, starts at eyes level and posteriorly to the medial line of the body, converges dorsally, and continues alongside the base of the dorsal fin until the middle third of the tail; medial line starts posteriorly to the posterior infraorbital line, 16–21 stitches runs dorsally across the body until it reaches the tail, at that point the stitches occur close to the axis of the tail myotomes, until the middle third, where it converges to the base of the dorsal fin and runs through its posterior third, number of stitches at the tail indistinguishable.

Buccopharyngeal cavity

Buccal roof (Fig. 4A–C): buccal roof triangular, longer than wide; prenarial arena almost twice as long as wide, with three longitudinal ridges, two larger located laterally, running through the posterior third to the middle third of the arena, and a smaller one located between the two larger ones. Choanae elongated and slit-shaped, located at an angle of 45° from the transverse plane, positioned at a distance of about 30% from the jaw sheath to the esophagus; anterior wall tall and robust, bearing one to two pairs of pustules and two pairs of filiform papillae, which present as a big pair over a smaller one; posterior wall tall and robust; narial valve visible, covering almost the entire nostril; maximum length of choanae and internarial distance representing about 30% and 15%, respectively, of the total width of the buccal roof. Postnarial arena length about 40% of the prenarial arena length, with almost 25 postnarial conical papillae, arranged as an inverted 'V' that runs from the central area to close to the lateral ridge papillae; three additional small postnarial papillae, arranged in a triangular shape located anteriorly to the median ridge. Median ridge crescent-shaped, located at a distance of about 45% from the jaw sheath to the esophagus, with six to eight secondary projections along its anterior edge. A pair of lateral ridge papillae present, with five hand-shaped secondary projections pointing towards the centre of the postnarial arena. Buccal roof arena (BRA) U-shaped, delimited anteriorly by the median ridge, laterally by about 25 smooth conical papillae of varied sizes, and posteriorly by about ten small, smooth and sparsely distributed conical papillae; BRA surface covered by a large amount of pustulations; about ten pairs of irregularly scattered papillae on the lateral portions of the buccal roof. Glandular zone distinct, arch-shaped, interrupted medially, wider in its lateral

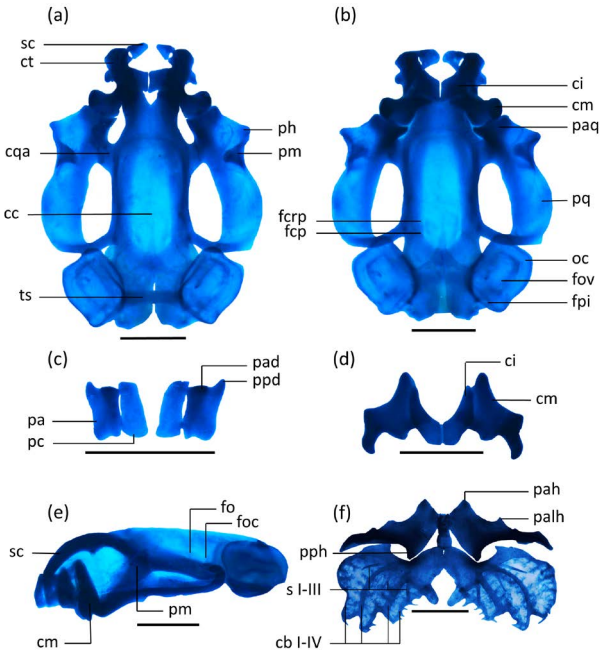

Figure 5. Skeleton of *Crossodactylus dantei* tadpole (MHNUFAL 12051, 12054) at stage 25 (Gosner, 1960; scale bar = 1 mm). Chondrocranium in **(A)** dorsal, **(B)** ventral, and **(E)** lateral views; **(C)** cartilago suprarostralis and **(D)** cartilago infrarostralis in frontal view, **(F)** hyobranchial apparatus in dorsal view. Abbreviations: cb I–IV = ceratobranchials I–IV; cc = cavum crani; ci = cartilago infrarostralis; cm = cartilago Meckeli; cqa = comissura quadratocranialis anterior; ct = cornua trabeculae; fcp = foramen caroticum primarium; fcrp = foramen craniopalatinum; fo = foramen opticum; foc = foramen oculotomotorium; fov = fenestra ovalis; fpi = foramen perilymphaticum inferior; oc = otic capsule; pa = pars alaris; pad = processus anterior dorsalis; pah = processus anterior hyalis; palh = processus anterolateralis hyalis; paq = pars articularis quadrati; pc = pars corporis; ph = processus hyalis; pm = processus muscularis; ppd = processus posterior dorsalis; pph = processus posterior hyalis; s I–III = spicules; pq = palatoquadrate; sc = suprarostral cartilage; ts = tectum synoticum.

portion, about 3% of the total length of the buccal roof. Dorsal velum about 6% of the buccal roof's total length, interrupted medially, with eight to nine large finger-shaped projections on each side.

Buccal floor (Fig. 4D & E): buccal floor triangular, slightly wider than long. Two pairs of infralabial papillae, the largest pair hand shaped and bear about 6 projections, they are arranged in a way that allow them to intertwine with the projections from the opposite pair; the smaller pair composed by conical papillae, located posteroventrally to the largest pair and covered by its projections. Lingual anlage bearing four conical lingual papillae of similar sizes distributed in an arc shape. Buccal floor arena (BFA) ellipsoid, surrounded by about 70 conical papillae that point towards the centre of the arena, arranged in 'U' shape, with abundant papillae on its lateral portion, with only around ten small papillae scattered on its posteromedial portion, largest papillae hand-shaped, bear about five finger-like projections, and found medially on the lateral portion; BFA surface covered by a large number of pustules. Buccal pockets oriented transversely, slit-shaped, about 15% of the size of the buccal floor and with three to four pairs of conical prepocket papillae. Ventral velum about 3% of the total length of the buccal floor, bears about eight conical projections on its margin, and a small irregular projection on its medial portion.

Larval skeleton

Chondrocranium elliptical in dorsal view and depressed in lateral view, higher at the level of pars articularis quadrati and wider in the middle third of palatoquadrate (Fig. 5A & E).

Suprarostral cartilage divided into pars alaris and pars corporis, both united by cartilaginous tissue dorsally and ventrally, forming a large foramen centrally; pars alaris quadrangular, wide and robust, processus posterior dorsalis flat and triangular, processus anterior dorsalis small and robust; pars corporis flat and rectangular, with no connections between them (Fig. 5C). Cornua trabeculae V-shaped and appears from planum trabeculare anticum, corresponding to 25% of chondrocranium length; processus lateralis trabeculae conspicuous at the posteroventral portion of each trabeculae; planum trabeculare anticum wider than long. Cranial floor occluded by a thin layer of cartilage, foramina carotica primaria and craniopalatina visible at its posterior portion, the latter larger than the former; orbital cartilage partially chondrified, foramina opticum and oculomotorium small. Tectum synoticum approximately 5% of chondrocranium length. Taenia tecti marginalis confluent with otic capsules.

Otic capsules quandrangular, about 30% of chondrocranium length; fenestra ovalis square-shaped, about 15% of chondrocranium length, situated in the medial portion of the otic capsules. Crista parotica inconspicuous, bearing a small processus anterolateralis. Arcus occipitalis protruding posterolaterally from the otic capsules. Foramen jugulare and foramen perilymphaticum present at the posteromedial portion of the otic capsules, the latter much larger than the former. A notch, representing 20% of chondrocranium length, marks the insertion point of notochord into the planum basale.

Palatoquadrate wide, expanding laterally in its posterior portion, with a dorsal curvature that connects to the orbital cartilage through the processus ascendens; lateral margin convex in dorsal view, and flat in lateral view, subocular arch with a smooth margin; processus ascendens attached to chondrocranium at the orbital cartilage, below the level of foramen oculomotorium (low suspensorium). Palatoquadrate attached to chondrocranium anteriorly through commissura quadratocranialis anterior; processus quadratoethmoidalis inconspicuous; processus pseudopterygoideus absent; processus antorbitalis inconspicuous; processus muscularis quadrati small,

Table 2. Acoustic traits of the advertisement and territorial calls of *Crossodactylus dantei*. Data presented as mean ± standard deviation (range).

Call traits	Advertisement call	Territorial call	Note A	Note B
Calls	14	3		
Calls/minute	0.85	0.15		
Call duration (s)	2.5 ± 0.13 (2.3–2.7)	23.16 ± 6.5 (18–30.5)		
Intercall interval (s)	61 ± 39 (15–143)			
Notes/call	22.8 ± 1.2 (21–25)	26.6 ± 11.5 (15–38)	16.3 ± 8 (0–25)	10.3 ± 3.7 (6–13)
Note duration (ms)	44 ± 18 (5.2–90.6)	134.9 ± 84 (33.8–324.8)	72.4 ± 15.8 (33.8–105.3)	233.6 ± 42 (94–324.8)
Pulses/note	15.2 ± 6.75 (2–35)	20.5 ± 7.82 (7–38)	25 ± 7.7 (10–38)	13.2 ± 1.9 (7–17)
Internote interval (ms)	70.4 ± 20.3 (17.3–190)	390.3 ± 281.1 (94–1141.2)		
Dominant frequency (Hz)	3356 ± 564 (1636–6546)	3160 ± 635 (2239–4134)	3452 ± 616 (2239–4134)	2690 ± 401 (2239–3617)

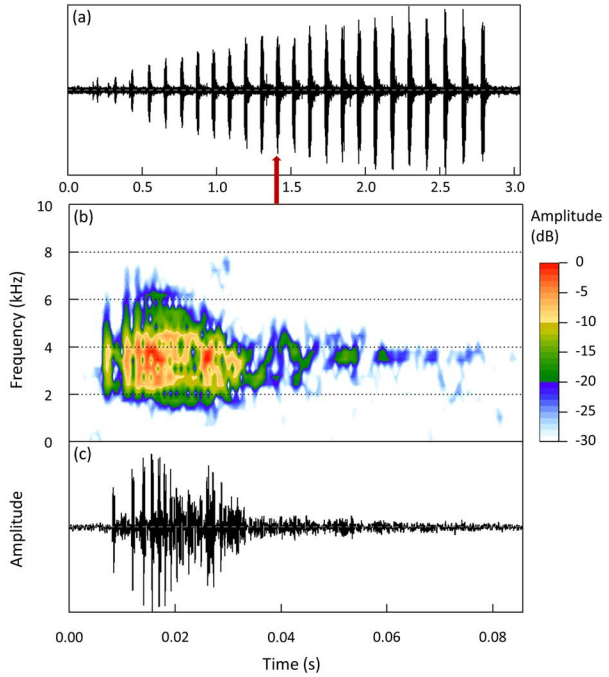

Figure 6. **(A)** Oscillogram of the advertisement call of *Crossodactylus dantei* (MHNUFAL 11934), followed by **(B)** a spectrogram and **(C)** corresponding oscillogram of one the notes identified by a red arrow.

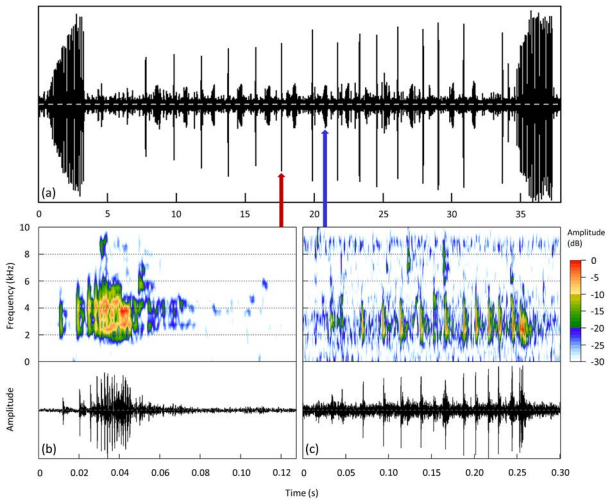

Figure 7. **(A)** Oscillogram of a territorial call emitted amid advertisement calls by *Crossodactylus dantei* (MHNUFAL 11934), followed by a spectrogram and corresponding oscillogram of **(B)** atype A note (identified by a red arrow) and **(C)** a type B note (identified by a blue arrow).

triangular, with rounded tip, curved medially, pointing towards processus antorbitalis; facies articularis hyalis relatively large and rounded, located at the posterior portion of the connection between the processus muscularis quadrati and the palatoquadrate. Pars articularis quadrati square-shaped and robust, forming the anterior portion of the palatoquadrate, with a ventral curvature.

Cartilago meckeli robust, transversely oriented, at an angle of approximately 80° to the main axis of the body; processus retroarticularis robust, with a curvature that embraces the pars articularis quadrati; processus dorsomedialis larger than processus ventromedialis. Cartilago infrarostralis sickle-shaped, longer than wide, fused medially by a thin layer of connective tissue, which can be U-shaped in dorsal view (Fig. 5B & D).

Ceratohyal elongated, oriented perpendicularly to the chondrocranium; processus anterior hyalis larger than processus anterolateralis hyalis, both triangular; processus posterior hyalis large, with a rounded margin; copula anterior absent; pars reuniens small and square-shaped; copula posterior small, longer than wide; processus urobranchialis inconspicuous. Hypobranchial plates ovoid, fused medially, posterior margins diverging in an inverted 'U' shape; processus anterior branchialis large, triangular, medially pointed; ceratobranchials confluent with the hypobranchial plate, ceratobranchialis I and II smaller than the others; spicules evident; processus branchialis 'open' (Fig. 5F).

Vocalisations

The advertisement call of *C. dantei* is formed by a sequence of notes emitted as short energy bursts in a brief time interval, each interspersed with well-defined silences (Fig. 6). The call exhibits an ascendant amplitude modulation, in which the duration and intensity of the notes progressively increase over time, occasionally slightly fading before the end. Each note consists of partially fused pulses, where the first pulse is often followed by a short silent period. In a single recording

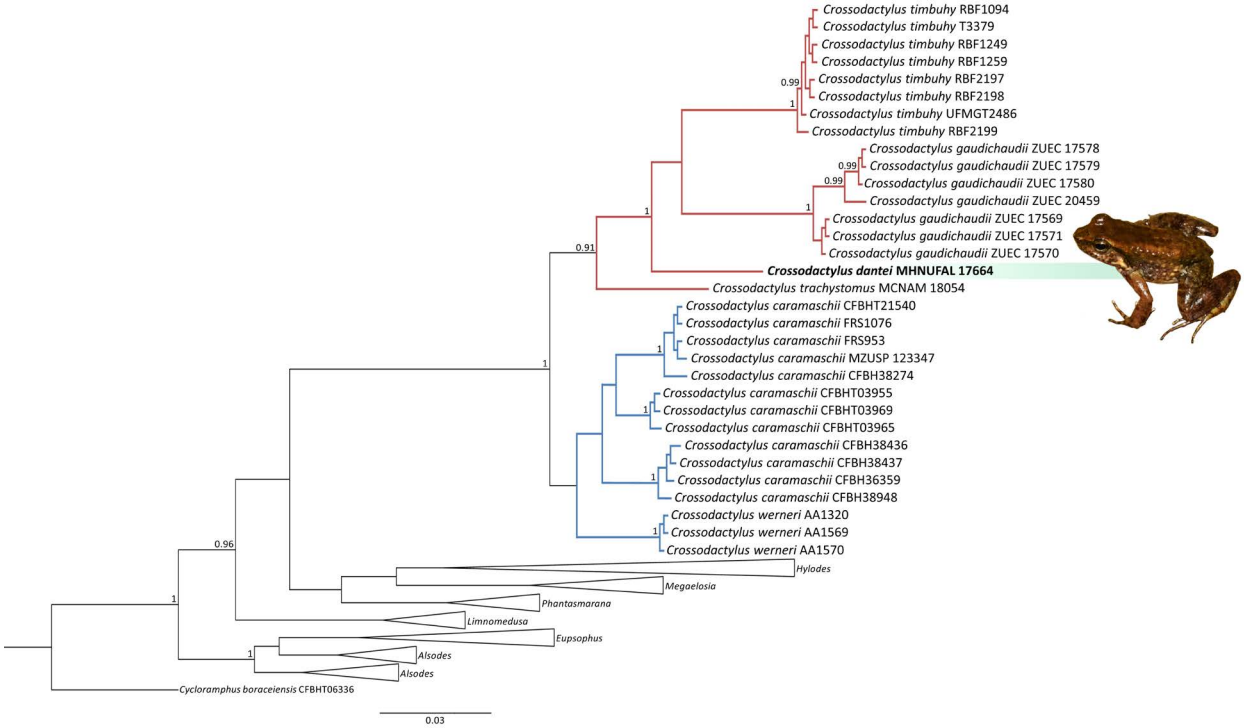

Figure 8. Bayesian Inference phylogram of the 16S rRNA Mitochondrial gene fragment for Hylodidae and Alsodidae families with nodes showing posterior probabilities > 0.90. Coloured branches represent different clades within *Crossodactylus.*

Table 3. Genetic distances between and within (intra) species belonging to the *Crossodactylus* genera. Estimated using Kimura 2-parameters evolutionary model (K2P) with complete deletion of gaps in the 16S rRNA mitochondrial gene fragment.

K2P	*C. dantei*	*C. gaudichaudii*	*C. caramaschii*	*C. timbuhy*	*C. trachystomus*	*C. werneri*	Intra
C. dantei	-						-
C. gaudichaudii	0.095	-					0.01
C. caramaschii	0.097	0.101	-				0.03
C. timbuhy	0.092	0.116	0.088	-			0
C. trachystomus	0.092	0.100	0.080	0.109	-		-
C. werneri	0.115	0.126	0.062	0.105	0.081	-	0

of nearly 17 minutes, 14 instances of an advertisement call were registered (Table 2). Each call lasted 2.5 ± 0.13 s (2.3–2.7 s) and consisted of 22.8 ± 1.2 (21–25) notes, each lasting 44 ± 18 ms (5.2–90.6 ms) and separated by silent intervals of 70.4 ± 20.3 ms (17.3–190 ms). The dominant frequency was 3356 ± 564 Hz (1636–6546 Hz). Harmonics may be discernible, but the recording quality precluded definitive identification of their precise spectral characteristics. The call can be classified as a "pulse repetition" according to Beeman's (1998) sound categories.

A distinct vocalisation was also recorded, which was categorised as territorial call based on a combination of acoustic analysis and field observations of social context. It consists of a complex call characterised by the presence of two different note types: one short, with partly fused pulses (type A); and the other long, with pulses separated by silent intervals (type B). These notes tend to occur in an alternating manner, interspersed by long intervals of silence, with ascendant amplitude modulation. Three territorial calls were recorded across three different recordings that totaled approximately 19 minutes, one of these calls was emitted amid a series of advertisement calls (Fig. 7, Table 2). The territorial call lasts 23.16 ± 6.5 s (18–30.5 s) and is composed of 26.6 ± 11.5 (15–38) notes, of which 16.3 ± 8 (0–25) are type A and 10.3 ± 3.7 (6–13) type B. The dominant frequency was 3160 ± 635 Hz (2239–4134 Hz), with type B notes exhibiting a lower mean frequency [2690 ± 401 Hz (2239–3617 Hz)] than type A notes [3452 ± 616 Hz (2239-4134 Hz)].

Phylogenetic position

The final alignment resulted in a matrix of 756 base pairs. The GTR+G evolutionary model was selected by PartitionFinder as the most appropriate for our dataset. Phylogenetic analysis recovered the genus *Crossodactylus* as monophyletic, with two major sister clades (PP = 1; GD = 0.09). The first clade consisted of *C. timbuhy*, *C. gaudichaudii*, *C. dantei* and *C. trachystomus*; while the second clade comprised *C. caramaschii* and *C. werneri*

(Fig. 8). In the first clade, *C. trachystomus* was recovered as the most external species, while *C. dantei* was found to be a sister species to a clade (PP = 1) composed of *C. gaudichaudii* (GD = 0.09) and *C. timbuhy* (GD = 0.09). Refer to Table 3 for genetic divergence values.

DISCUSSION

Tadpole morphology

Crossodactylus larvae have a highly conserved body plan, which may result from analogous ecological pressures exerted by their specialised microhabitat (Caramaschi & Kisteumacher, 1989; Toscano et al., 2019). Typically, these tadpoles occupy the backwaters of fast-flowing streams, that are characterised by sandy or muddy substrates, rocks and abundant tree litter. These species exhibit benthic and cryptic habits, often swimming near the bottom and using the substrate, leaves, rocks and crevices as sources of camouflage and shelter (e.g. Caramaschi & Kisteumacher, 1989; Silva-Soares et al., 2015; Toscano et al., 2019; de Sá et al., 2022; Lacerda et al., 2022). The external morphology of *Crossodactylus* tadpoles is typically characterised by an ovoid or elliptical body in dorsal view, rounded snout, eyes and nostrils dorsally or dorsolaterally positioned, a short sinistral spiracle posterodorsally oriented, dextral vent tube, oral disc ventrally positioned, jaw sheaths robust, LTRF 2(2)/3(1), colouration brown or beige with melanophores scattered along the tail.

Only *Crossodactylus cyclospinus*, *C. dantei* and *C. gaudichaudii* exhibit an elliptical body shape in dorsal view (Nascimento et al., 2005; Silva-Soares et al., 2015), with the remaining species in the genus presenting ovoid bodies; except for *C. schmidti*, whose dorsal body has been described as "subovoid" (Faivovich, 1998). Among those with an elliptical body shape, *C. dantei* stands out for being the only one with its nostrils positioned closer to the snout than the eyes. Furthermore, *C. dantei* and *C. cyclospinus* have an emarginated oral disc, while only *C. cyclospinus* possesses an incised upper jaw sheath. Consequently, *C. dantei* can be distinguished from *C. cyclospinus* by its non-incised upper jaw sheath, from *C. gaudichaudii* by its emarginated oral disc, and from the remaining species in the genus by its elliptical body shape in dorsal view. In lateral view, *C. dantei* has a considerably more elongated and depressed body compared to its congeners; however, certain specimens may bear a resemblance in lateral view to *C. gaudichaudii* due to a similar body shape (Silva-Soares et al., 2015).

Another shared feature in *Crossodactylus* species is the presence of a distinct lateral line system. Francioni & Carcerelli (1993) reported the absence of a distinct lateral line system in *C. gaudichaudii*, although Silva-Soares et al. (2015) did not explicitly mention the presence of a lateral line system in this species (as *C. aeneus*), the system seems discernible in the provided images, suggesting that *C. gaudichaudii* has a distinct lateral line system.

Crossodactylus gaudichaudii, *C. trachystomus* and *C. caramaschii* are the only ones with documented buccopharyngeal anatomy (Haas, 2003; Weber & Caramaschi, 2006; Toscano et al., 2019). Although these species display remarkable similarities, distinct traits can still be observed in *C. dantei*. Notably, *C. dantei* exhibits three longitudinal ridges in the prenarial arena, whereas other species either lack visible structures (*C. trachystomus*) or possess inconspicuous ones (e.g. a single tiny pustulation in *C. caramaschii*, a faint longitudinal ridge in *C. gaudichaudii*). Moreover, we reported the occurrence of two pairs of filiform papillae on the choanae anterior wall of *C. dantei*, whereas the remaining species either have one pair (*C. gaudichaudii*, *C. trachystomus*) or none (*C. caramaschii*). Weber & Caramaschi (2006) suggested that the morphology of the ventral velum constitutes a crucial taxonomic trait for the genus, probably due to its variations. Curiously, the ventral velum of *C. dantei* bears striking resemblance to that of *C. gaudichaudii.*

The chondrocranial morphology was only reported for *C. gaudichaudii* (Silva-Soares et al., 2015). In fact, descriptions of larval skeletons are rare in the family Hylodidae, and to date, they only exist for *Hylodes meridionalis* (Mertens, 1927), described by Nogueira-Costa & Wachlevski (2015), *H. ornatus* (Bokermann, 1967), described by Bilate et al. (2012), and *H. pipilans* Canedo & Pombal, 2007, described by Nogueira-Costa et al. (2017). It has been observed that the chondrocranium of this family is highly comparable across species, indicating the conservative nature of this characteristic within this family, as suggested by Nogueira-Costa & Wachlevski (2015). Despite the limited number of larval skeleton characterisations, trait variation was still observed between *Hylodes* and *Crossodactylus*. *Hylodes* possesses a pair of adrostral cartilages, which are absent in *Crossodactylus*; the processus muscularis is more extensively developed in *Hylodes* compared to *Crossodactylus*; and the processus anterolateralis hyalis is more developed in *Crossodactylus* compared to *Hylodes* (Nogueira-Costa & Wachlevski, 2015; Bilate et al., 2012; Silva-Soares et al., 2015). Among *Crossodactylus*, the absence of taenia tecti medialis and taenia tecti transversalis in *C. dantei* differentiates it from *C. gaudichaudii*, in which these features are present (Silva-Soares et al., 2015).

Vocalisations

The advertisement call of *C. dantei* follows the pattern observed in non-mute Hylodidae, as a trill with short, high-pitched, quickly repeated notes. This structure is attributed to the presence of a noisy environment generated by fast-torrent streams, which has driven the evolution of high-pitched calls that effectively surpass background noise (Haddad & Giaretta, 1999; Lingnau & Bastos, 2007). Notably, *C. dantei* exhibits an ascending amplitude modulation, a characteristic shared with other *Crossodactylus* species such as *C. trachystomus*, *C. franciscanus*, *C. werneri* and *C. timbuhy* (Pimenta et al., 2008; 2015; Vidigal et al., 2018; Lacerda et al., 2022); however, the emission of isolated notes between calls, which has been reported in other *Crossodactylus* species (Pimenta et al., 2015; Vidigal et al., 2018),

was not observed in *C. dantei.* The advertisement call of *C. dantei* can be distinguished from those of its congeners by the presence of a distinct set of extreme traits that are unique to this species. *Crossodactylus dantei* (21–25 notes) and *C. werneri* (12–25 notes) have the lowest number of notes per call (Vidigal et al., 2018). *Crossodactylus dantei* (5.2–90.6 ms) and *C. gaudichaudii* (40–50 ms) produce the longest notes on average (Weygoldt & Silva, 1992). Additionally, *C. dantei* has the shortest advertisement call in the genus. The mean call frequency is comparable to that of *C. werneri*, the species with the lowest-frequency call (Vidigal et al., 2018); considering the similarity in snout-vent length (SVL) between both species, these results align with the conclusions of Augusto-Alves et al. (2021), who established a correlation between the dominant frequency of advertisement calls and SVL in Hylodidae.

Territorial calls have been documented for *C. gaudichaudii, C. cyclospinus, C. schmidti, C. werneri* and *C. timbuhy* (Weygoldt & Silva, 1992; Nascimento et al., 2005; Caldart et al., 2012; Vidigal et al., 2018; Lacerda et al., 2022). Of these, only *C. dantei* and *C. timbuhy* have been observed to emit two distinct notes in an alternating pattern during territorial behaviour. Both calls consist of a long note, with ascending amplitude modulation and pulses separated by silent intervals, and a short note, with partially fused pulses. However, it is possible to differentiate the territorial call of *C. dantei* from *C. timbuhy* based on the shorter mean duration of its long note (*C. dantei* = 233.6 ms vs. *C. timbuhy* = 400 ms), and the lower dominant frequency of both short and long notes (*C. dantei* χ = 3.4 kHz and χ = 2.6kHz vs. *C. timbuhy* χ = 3.7 kHz and χ = 3.4 kHz).

Phylogenetic position

Despite being constructed based on a single-gene dataset, we present one of the most comprehensive phylogenetic trees for the genus *Crossodactylus* to date. Our analyses revealed a basal split within the genus, resulting in the formation of two major clades.

Our findings differed from previous work (Toscano et al., 2019; Vittorazzi et al., 2021; de Sá et al., 2022) that recovered *C. trachystomus* as sister taxon of *C. caramaschii* + *C. werneri*, instead, we found strong statistical support (PP = 0.91) for *C. trachystomus* as sister taxon to a clade composed of *C. dantei* + *C. gaudichaudii* + *C. timbuhy*.

Crossodactylus caramaschii and *C. werneri* were recovered as sister species, as previously reported (Toscano et al., 2019; Vittorazzi et al., 2021; de Sá et al., 2022). Additionally, *C.caramaschii* is structured into three distinct mitochondrial lineages (GD = 0.03), suggesting that this taxon may represent a species complex (Fabri, 2013; Toscano et al., 2019).

Recently, Portik et al. (2023) developed a comprehensive phylogenetic hypothesis for anurans, based on more than 5000 species, including six representatives of the genus *Crossodactylus*. In comparison to the present study, its molecular data matrix incorporated *C. schmidti* instead of *C. dantei*, and multiple loci instead of just one. The resulting final topology highlights a basal dichotomy between *C. schmidti* and the other species of the genus, which in turn, exhibit a topology similar to that presented herein.

Toscano et al. (2019), Vittorazzi et al. (2021) and de Sá et al. (2022) present *Crossodactylus* topologies that are very similar to each other but are slightly different from those obtained by Portik et al. (2023) and in the present study. Although these works use a larger molecular data set, Toscano et al. (2019) exclusively used the 16S gene. A common factor that differentiates them from the current study, as well as from Portik et al. (2023), is the absence of *C. timbuhy* and significantly smaller outgroups (For a comprehensive view of the outgroup, refer to Figure S1 in supplementary material). Whereas Portik et al. (2023) also included in their analysis the markers used in the previously cited literature, factors such as the number of species of the genus *Crossodactylus* included in the analysis, and possibly the number of species in the outgroup, seem to be important for the topology obtained by the current work.

ACKNOWLEDGEMENTS

Collection permits were issued by Instituto Chico Mendes de Conservação da Biodiversidade (ICMBio/SISBIO n° 33507-1). We thank Nelma Mendonça (IBAMA), chief of ESEC Murici and her team, for the permission and logistical support in the fieldwork.

REFERENCES

Augusto-Alves, G., Dena, S. & Toledo, L.F. (2021). Acoustic allometry, background stream noise and its relationship with large-bodied and voiceless rheophilic frogs. *Zoologischer Anzeiger* 295, 156–162.

Altig, R. & Johnston, G.F. (1989). Guilds of anuran larvae: Relationships among developmental modes, morphologies, and habitats. *Herpetological Monographs* 3, 81.

Bastos, R.P. & Pombal, J.P. (1995). New species of *Crossodactylus* (Anura: Leptodactylidae) from the Atlantic rain forest of southeastern Brazil. *Copeia* 436–439.

Beeman, K. (1998). Digital signal analysis, editing, and synthesis. *Animal acoustic communication: sound analysis and research methods* 59–103.

Bilate, M., Nogueira-Costa, P. & Weber, L.N. (2012). The tadpole of the hylodid frog *Hylodes ornatus* (Bokermann, 1967), including chondrocranium description, and advertisement call. *Zootaxa* 3249(1), 60–66.

Caldart, V., Iop, S., Cechin, S. & Bertaso, T. (2012). Feeding ecology of *Crossodactylus schmidti* (Anura: Hylodidae) in Southern Brazil. *Zoological studies* 51, 484–493.

Caramaschi, U. & Kisteumacher, G. (1989). O girino de *Crossodactylus trachystomus* (Reinhardt and Luetken, 1862) (Anura, Leptodactylidae). *Revista Brasileira de biologia* 49(1), 237–239.

de Sá, F.P., Condez, T.H., Lyra, M.L., Haddad, C.F. & Malagoli, L.R. (2022). Unveiling the diversity of Giant Neotropical Torrent frogs (Hylodidae): phylogenetic relationships, morphology, and the description of two new species. *Systematics and*

Biodiversity 20(1), 1–31.

Dingerkus, G. & Uhler, L.D. (1977). Enzyme clearing of alcian blue stained whole small vertebrates for demonstration of cartilage. *Stain Technology* 52(4), 229–232.

Fabri, D.A. (2013). Molecular phylogenetics of *Crossodactylus* Duméril & Bibron, 1841 (Anura: Hylodidae) (Master's thesis, Pontifícia Universidade Católica do Rio Grande do Sul).

Faivovich, J. (1998). Comments on the larvae of the Argentine species of the genus *Crossodactylus* (Leptodactylidae, Hylodinae). *Alytes Paris* 16, 61–67.

Francioni, E. & Carcerelli, L.C. (1993). Descrição do girino de *Crossodactylus gaudichaudii* Duméril & Bibron, 1841 (Anura, Leptodactylidae). *Memórias do Instituto Butantan* 55(1), 63–67.

Frost, D.R. (2023). Amphibian Species of the World: an Online Reference, Version 6.1. Downloaded on 24 April 2023. Doi. org/10.5531/db.vz.0001 https://amphibiansoftheworld. amnh.org/index.php.

Grant, T. (2019). Outgroup sampling in phylogenetics: Severity of test and successive outgroup expansion. *Journal of Zoological Systematics and Evolutionary Research* 57(4), 748–763.

Gosner, K.L. (1960). A simplified table for staging anuran embryos and larvae with notes on identification. *Herpetologica* 16(3), 183–190.

Grosjean, S. (2005). The choice of external morphological characters and developmental stages for tadpole-based anuran taxonomy: A case study in *Rana* (Sylvirana) *nigrovittata* (Blyth, 1855) (Amphibia, Anura, Ranidae). *Contributions to Zoology* 74(1–2), 61–76.

Haas, A. (2003). Phylogeny of frogs as inferred from primarily larval characters (Amphibia: Anura). *Cladistics* 19(1), 23–89.

Haddad, C.F. & Giaretta, A.A. (1999). Visual and acoustic communication in the Brazilian torrent frog, *Hylodes asper* (Anura: Leptodactylidae). *Herpetologica* 324–333.

Hall, T.A. (1999). BioEdit: a user-friendly biological sequence alignment editor and analysis program for Windows 95/98/ NT. *Nucleic acids symposium series* 41(41), 95–98.

K. Lisa Yang Center for Conservation Bioacoustics at the Cornell Lab of Ornithology. (2023). Raven Pro: Interactive Sound Analysis Software (Version 1.6.4) [Computer software]. Ithaca, NY: The Cornell Lab of Ornithology. Available from https://ravensoundsoftware.com/.

Katoh, K. & Standley, D.M. (2013). MAFFT multiple sequence alignment software version 7: improvements in performance and usability. *Molecular biology and evolution* 30(4), 772–780.

Kimura, M. (1980). A simple method for estimating evolutionary rates of base substitutions through comparative studies of nucleotide sequences. *Journal of molecular evolution* 16, 111–120.

Köhler, J., Jansen, M., Rodríguez, A., Kok, P.J.R., Toledo, L.F., Emmrich, M., Glaw, F., Haddad, C.F.B., Rödel, M.-O. & Vences, M. (2017). The use of bioacoustics in anuran taxonomy: Theory, terminology, methods and recommendations for best practice. *Zootaxa* 4251(1), 1.

Kumar, S., Stecher, G., Li, M., Knyaz, C. & Tamura, K. (2018). MEGA X: molecular evolutionary genetics analysis across computing platforms. *Molecular biology and evolution* 35(6), 1547.

Lacerda, J.V.A., Montesinos, R., Zocca, C., Guimarães, C.S., Santana, D.J. & Ferreira, R.B. (2022). On the stream-dwelling *Crossodactylus timbuhy* (Anura, Hylodidae): Taxonomy, natural history, and geographic distribution. *Zootaxa* 5155(4), 564–580.

Laia, R.C. & Rocha, C.F.D. (2012). Adults and tadpoles of species of Hylodidae (Anura): history and taxonomy perspectives. *Zoologia (Curitiba)* 29(1), 89–94.

Lanfear, R., Calcott, B., Ho, S.Y. & Guindon, S. (2012). PartitionFinder: combined selection of partitioning schemes and substitution models for phylogenetic analyses. *Molecular biology and evolution* 29(6), 1695–1701.

Larson, P.M. & de Sá, R.O. (1998). Chondrocranial morphology of *Leptodactylus* larvae (Leptodactylidae: Leptodactylinae): Its utility in phylogenetic reconstruction. *Journal of Morphology* 238(3), 287–305.

Lavilla, E.O. & Scrocchi, G.J. (1986). Morfometría larval de los géneros de Telmatobiinae (Anura: Leptodactylidae) de Argentina y Chile. *Physis* 44(106), 39–43.

Lingnau, R. & Bastos, R.P. (2007). Vocalizations of the Brazilian torrent frog *Hylodes heyeri* (Anura: Hylodidae): Repertoire and influence of air temperature on advertisement call variation. *Journal of Natural History* 41(17–20), 1227–1235.

Lyra, M.L., Haddad, C.F. & de Azeredo-Espin, A.M.L. (2017). Meeting the challenge of DNA barcoding Neotropical amphibians: polymerase chain reaction optimization and new COI primers. *Molecular Ecology Resources* 17(5), 966–980.

McDiarmid, R.W. & Altig, R. (1999). Tadpoles: The Biology of Anuran Larvae. University of Chicago Press. 444 p.

Nascimento, L.B., Cruz, C.A.G. & Feio, R.N. (2005). A new species of Diurnal Frog in the genus *Crossodactylus* Duméril and Bibron, 1841 (Anura, Leptodactylidae) from Southeastern Brazil. *Amphibia-Reptilia* 26(4), 497–505.

Nogueira-Costa, P. & Wachlevski, M. (2015). The tadpole of *Hylodes meridionalis* (Mertens, 1927), a lotic stream anura from the Atlantic Rainforest of Brazil. *Zootaxa* 4032(2), 199–202.

Nogueira-Costa, P., Weber, L.N., Wogel, H., Salles, R.O.L. & Bilate, M. (2017). A description of the tadpoles of *Hylodes pipilans* Canedo & Pombal, 2007: An endemic species of the Atlantic Forest of Brazil. *Herpetological Conservation and Biology* 14(2), 370–379.

Pimenta, B.V., Caramaschi, U. & Cruz, C.A.G. (2015). Synonymy of *Crossodactylus bokermanni* Caramaschi & Sazima, 1985 with *Crossodactylus trachystomus* (Reinhardt & Lütken, 1862) and description of a new species from Minas Gerais, Brazil (Anura: Hylodidae). *Zootaxa* 3955(1), 65–82.

Pimenta, B.V., Cruz, C.A.G. & Caramaschi, U. (2014). Taxonomic Review of the species complex of *Crossodactylus dispar* A. Lutz, 1925 (Anura, Hylodidae). *Arquivos de Zoologia* 45(1), 1.

Pimenta, B.V., Wachlevski, M. & Cruz, C.A.G. (2008). Morphological and acoustical variation, geographic distribution, and conservation status of the spinythumb frog *Crossodactylus bokermanni* Caramaschi & Sazima, 1985 (Anura, Hylodidae). *Journal of Herpetology* 42(3), 481–492.

Pinheiro, P.D.P., Pezzuti, T.L. & Garcia, P.C.A. (2012). The

tadpole and vocalizations of *Hypsiboas polytaenius* (Cope, 1870) (Anura, Hylidae, Hylinae). *South American Journal of Herpetology* 7(2), 123–133.

Portik, D.M., Streicher, J.W. & Wiens, J.J. (2023). Frog phylogeny: a time-calibrated, species-level tree based on hundreds of loci and 5,242 species. *Molecular Phylogenetics and Evolution* 188(107907).

R Core Team (2022). R: A language and environment for statistical computing. R Foundation for Statistical Computing, Vienna, Austria. https://www.R-project.org/.

Rodrigues, G.D.V., Nascimento, F.A.C., Almeida, J.P.F.A. & Mott, T. (2017). The tadpole of *Scinax skuki* (Anura: Hylidae) from the type locality, with a description of its larval skeleton. *Studies on Neotropical Fauna and Environment* 52(3), 204–215.

Ronquist, F., Teslenko, M., van der Mark, P., Ayres, D.L., Darling, A., Höhna, S., Larget, B., Liu, L., Suchard, M.A. & Huelsenbeck, J.P. (2012). MrBayes 3.2: Efficient bayesian phylogenetic inference and model choice across a large model space. *Systematic Biology* 61(3), 539–542.

Sambrook, J., Fritsch, E.F. & Maniatis, T. (1989). Molecular cloning: a laboratory manual (No. Ed. 2). Cold Spring Harbor Laboratory Press.

Silva-Soares, T., Nogueira-Costa, P., Júnior, V.N.T.B., Weber, L.N. & Rocha, C.F.D. (2015). The Larva of *Crossodactylus aeneus* Müller, 1924: Morphology and Ecological Aspects. *Herpetologica* 71(1), 46–57.

Silvano, D. & Freire, E.M.X. (2004). *Crossodactylus dantei*. The IUCN Red List of Threatened Species 2004: e.T56350A11466595. Accessed on 30 May 2023. https://dx.doi.org/10.2305/IUCN.UK.2004.RLTS.T56350A11466595.en.

Sueur, J., Aubin, T. & Simonis, C. (2008). Seewave, a free modular tool for sound analysis and synthesis. *Bioacoustics* 18(2), 213–226.

Toscano, N.P., Freitas, N.H.A., Rezende, M.R.C., Provete, D.B., Lyra, M., Haddad, C.F.B., Rossa-Feres, D.C. & Silva, F.R. (2019). External morphology and internal oral features of the tadpole of *Crossodactylus caramaschii* (Anura: Hylodidae). *Journal of Herpetology* 53(4), 263.

Vera Candioti, M.F (2007). Anatomy of anuran tadpoles from lentic water bodies: systematic relevance and correlation with feeding habits. *Zootaxa* 1600(31), 1–175.

Vidigal, I., de Carvalho, T.R., Clemente-Carvalho, R.B.G. & Giaretta, A.A. (2018). Vocalizations, tadpole, and natural history of *Crossodactylus werneri* Pimenta, Cruz & Caramaschi, 2014 (Anura: Hylodidae), with comments on distribution and intraspecific variation. *Zootaxa* 4388(1), 61.

Vieira, W.L.S., de Moura, G.J.B., Júnior, F.V.M., Santana, G.G., Mott, T., Dubeux, M.J.M., Nascimento, F.A.C. & Vieira, K.S. (2023). Species richness, distribution pattern, and conservation of amphibians in the northern portion of the Brazilian Atlantic Forest. In *Animal Biodiversity and Conservation in Brazil's Northern Atlantic Forest*, Springer International Publishing. 147–167 pp.

Vittorazzi, S.E., Lourenço, L.B., Zattera, M.L., Weber, L.N., Recco-Pimentel, S.M. & Bruschi, D.P. (2021). Cytogenetic and genetic data support *Crossodactylus aeneus* Müller, 1924 as a new junior synonym of *C. gaudichaudii* Duméril and Bibron, 1841 (Amphibia, Anura). *Genetics and Molecular Biology* 44.

Wassersug, R.J. (1976). Oral morphology of anuran larvae: terminology and general description. *Occasional papers of the Museum of Natural History, The University Of Kansas* 48, 1–23.

Wassersug, R.J. (1980). Internal oral features of larvae from eight Anuran families: functional, systematic, evolutionary, and ecological considerations. *University of Kansas* 68, 146.

Weber, L.N. & Caramaschi, U. (2006). Descrição da morfologia oral interna de larvas do gênero *Crossodactylus* Duméril & Bibron, 1841 (Amphibia, Anura, Leptodactylidae). *Arquivos do Museu Nacional* 64(2), 141–149.

Wells, K.D. (2007). The Ecology and Behavior of Amphibians. University of Chicago press.

Weygoldt, P. & Silva, S.P.D.C. (1992). Mating and oviposition in the hylodine frog *Crossodactylus gaudichaudii* (Anura: Leptodactylidae). *Amphibia-Reptilia* 13(1), 35–45.

Accepted: 6 February 2024

Please note that the Supplementary Material for this article is available online via the Herpetological Journal website: https://thebhs.org/publications/the-herpetological-journal/volume-34-number-3-july-2024